Physisorption interaction of H_2 with noble-metal surfaces: A new H_2-Cu potential

S. Andersson and L. Wilzén
Department of Physics, Chalmers University of Technology, S-412 96 Göteborg, Sweden

M. Persson
Institute of Theoretical Physics, Chalmers University of Technology, S-412 96 Göteborg, Sweden
(Received 4 December 1987)

Using molecular beams of H_2 and D_2 with incident energies and angles in the ranges 5–50 meV and 40°–80°, we have measured diffractive selective adsorption scattering resonances from a Cu(100) surface kept at 80 K. From the dispersion relations—resonance energy versus incident angle—we have unambiguously identified the resonances and determined the appropriate bound-state level energies. We have analyzed these data and arrived at a level assignment that is compatible with a single gas-surface potential curve for H_2 and D_2. We find a well depth of 30.9 meV, which is substantially larger than the commonly accepted value around 22 meV for the H_2-Cu system. We note that our data strikingly resembled those reported for the H_2-Ag system and discuss these observations in relation to theoretical predictions.

I. INTRODUCTION

Physisorbed species of H_2, HD, and D_2 on cold surfaces of noble metals like Ag (Ref. 1) and Cu (Ref. 2) have been observed by high-resolution electron-energy-loss spectroscopy (HREELS). The HREELS spectra reveal rotational excitations and internal H—H stretch vibrational excitations that show minute shifts compared to gas-phase values, i.e., the molecule behaves like an essentially free three-dimensional (3D) rotor on these surfaces. This is unlike chemisorbed H_2 (Ref. 3) where the H—H stretch mode is substantially shifted towards lower energy and the rotational excitation is replaced by an antisymmetric stretch mode. In this case all the allowed dipole active modes related to the specific substrate H_2 configuration are observed. In the physisorption case, on the other hand, the spectroscopic measurements are not sensitive enough to reveal either vibrational excitations of H_2 in the physisorption potential well or any signature related to rotational hindering caused by any anisotropy in the H_2 metal interaction. This information has to be obtained by other means, in particular molecular-beam scattering experiments involving various kinds of resonant phenomena. Such experiments have been performed for H_2, HD, and D_2 scattered from single-crystal surfaces of Cu,[4,5] Ag,[6,7] and Au.[5] The measurements involve primarily detection of diffractive (or corrugation-mediated) selective adsorption resonances (CMSA) and rotationally mediated selective adsorption resonances (RMSA). Conventionally one or two beam energies are used and the resonances are detected by measuring, e.g., the intensity of the specular beam versus the angle of incidence with respect to the sample surface normal. A distinction between CMSA and RMSA resonances can be achieved by varying the azimuthal angle with respect to a given direction in the surface plane.[7] CMSA resonances depend on this angle while RMSA resonances do not. A particular high-resolution technique using velocity analysis of the scattered molecules and a broad primary-beam energy distribution has been used to detect RMSA resonances.[5] This method circumvents the problem of an intrinsically broad energy distribution of hydrogen nozzle beams ($\Delta\varepsilon/\varepsilon \geq 10\%$) and allows an energy resolution $\Delta\varepsilon/\varepsilon \approx 1-2\%$.

In this work we have used a new method to be able to assign resonance features unambigously. For fixed polar θ_i and azimuthal angles of incidence we scan the primary-beam energy ε_i over the range of interest and record the specular beam intensity. This procedure is repeated for a range of θ_i values. In this way we get a series of dispersion relations ε_i versus θ_i which easily can be identified with specific resonances via comparison with calculated dispersion curves. This fitting procedure gives the appropriate bound-state level energies. We have analysed these data according to the Rydberg-Klein-Rees method of molecular physics, as first discussed by LeRoy,[8] and found a level assignment that is compatible with a single gas-surface potential curve for H_2 and D_2. We arrive at a well depth of 30.9 meV for the H_2-Cu(100) physisorption potential, which is substantially larger than the commonly accepted value around 22 meV for the H_2-Cu system.[4,5] Ambiguities in the latter level assignments were recognized, however, and well depths in the range 31–32 meV were conceivable, i.e., in correspondence with our determination. The well depth we observe is very close to the value around 31.5 meV reported for the H_2-Ag system.[6,7] This is a notable observation in relation to recent theoretical calculations concerning the physisorption interaction of H_2 with noble metals.[9] These calculations predict a rather low well depth, 23.5 meV, for the H_2-Cu system and a clear difference between Cu and Ag. The theory is based on an model due to

Zaremba and Kohn[10] that the physisorption interaction is formed by the balance between the attractive van der Waal interaction and the repulsive interaction due to the overlap of the closed shell adsorbate with the substrate conduction electrons. We will discuss a few factors in these calculations that could bring this delicate balance between the attractive and repulsive part of the interaction in better agreement with the experimental observations.

II. EXPERIMENT

The equipment used in these experiments consisted of H_2 nozzle beams shaped by skimmers in three differentially turbopumped chambers operating at typical pressures of 1×10^{-3}, 1×10^{-6}, and 2×10^{-9} Torr, respectively. The gas was expanded from a 10-μm-diam nozzle source at temperatures between 20 and 300 K (combining liquid-helium cooling and resistive heating). The gas was precooled to liquid-nitrogen temperature before entering the nozzle source. The source temperature was electronically controlled via a thermocouple (Au+0.03 at. % Fe–Chromel) reading and could be kept steady or ramped linearly in time. H_2 pressures in the range 0.1–1.1 bars produced adequate molecular beams over the entire source temperature range with an optimum energy spread of $\approx$15%. The incident beam had an angular divergence of 0.25°.

The scattering experiments were performed in a cryopumped (1000 l/s) UHV system (UHV denotes ultrahigh vacuum) operating at a base pressure of 3×10^{-11} Torr, which increased to typically 3×10^{-10} Torr, when the beam was on. Primary and scattered beam intensities were measured with a rotatable stagnation arrangement (1.5° angular resolution) equipped with a calibrated ionization gauge. Diffraction measurements were carried out using this detection system and provided calibration of beam energy versus source temperature.

The Cu(100) sample was spark cut from a 99.999%-purity Cu single-crystal rod and oriented to better than 0.2°. The sample was subsequently mechanically and electrolytically polished to optimal optical finish and cleaned *in situ* by standard methods involving argon-ion bombardment and heating cycles. The sample could be cooled to 80 K (10 K) using liquid nitrogen (helium) as cooling agents and was heated resistively. It was mounted with respect to the direction of the incident molecular beam so that the scattering plane comprised the surface normal and the [010] direction in the surface.

In the resonance measurements described below, the specular beam intensity I_{00}, incident beam intensity I_0, and source temperature T_N were sampled, normalized, and plotted via a HP 200 series microcomputer and a HP7090A measurement plotting system. The Cu(100) specimen was kept at 80 K during the intensity versus T_N scans and was cleaned by a flash heating to 900 K between each measurement.

III. RESULTS AND DISCUSSION

Figure 1 shows two typical examples of normalized specular reflectivity, I_{00}/I_0, versus incident beam energy ε_i, at a fixed angle of incidence θ_i, obtained for H_2 and D_2 beams, respectively. Pronounced resonance structure is seen in the data, despite the fact that the Cu(100) surface is considered as "smooth" with respect to lateral corrugation. The resonance features shift in energy as the angle of incidence is varied. The energies of the resonance minima are plotted (open circle) versus θ_i in Figs. 2 and 3 for H_2 and D_2, respectively. We note that some weaker resonance features have been observed in the data. They disperse differently, however, than those plotted in Figs. 2 and 3, and are caused by inelastic events.

An unambigous identification of the resonances plotted in Figs. 2 and 3 in terms of CMSA resonances is provided by a kinematical analysis of their dispersion with respect to θ_i. The condition is simply that the energy ε_i and wave-vector component $\mathbf{K}_i$ parallel to the surface of the incident particle matches the energy $\varepsilon=\varepsilon_n+\hbar^2(\mathbf{K}_i+\mathbf{G})^2/(2m)$ of the particle trapped into a bound-state level n with energy $\varepsilon_n<0$, and that the wave-vector component parallel to the surface differs by a reciprocal surface lattice vector $\mathbf{G}$.[11] The corresponding set of discrete resonance energies $\varepsilon_{\mathrm{CMSA}}$ can be solved in a straightforward manner as a function of θ_i and are given by

$$\varepsilon_{\pm}=\varepsilon_G\left[\frac{\cos\phi\tan\theta_i\pm\left[\frac{\varepsilon_n}{\varepsilon_G}+1+\cos^2\phi\tan^2\theta_i\right]^{1/2}}{\cos\theta_i}\right]^2,$$

$$\varepsilon_{\mathrm{CMSA}}=\varepsilon_+,\varepsilon_- \quad \text{if } -\varepsilon_G(1+\cos^2\phi\tan^2\theta_i)<\varepsilon_n<-\varepsilon_G, \quad (1)$$

$$\varepsilon_{\mathrm{CMSA}}=\varepsilon_+ \quad \text{if } -\varepsilon_G<\varepsilon_n.$$

Here $\varepsilon_G=\hbar^2G^2/(2m)$ and $\cos\phi=\mathbf{K}_i\cdot\mathbf{G}/(KG)$. Note that if none of these inequalities are fulfilled, both ε_+ and ε_- are complex and accordingly do not correspond to any resonances. This formula applies also to the more general situation of selective adsorption resonances if ε_n is reinterpreted and if $\mathbf{G}=\mathbf{0}$ is included, e.g., in the case of RMSA resonances ε_n also includes the rotational energy of the trapped particle.

The solid curves in Figs. 2 and 3 represent kinematical CMSA resonance conditions involving the $\mathbf{G}_{10}$ surface reciprocal-lattice vectors. The curves were calculated from Eq. (1) and were fitted to the experimental data by adjusting the bound-state level energies ε_n (given at each curve). Higher order $\mathbf{G}$'s give markedly different dispersion relations due to different ε_G and $\cos\phi$, and can therefore immediately be ruled out. The accuracy of the fits in Figs. 2 and 3 gives an uncertainty of the ε_n values of order 0.1–0.2 meV.

The kinematical analysis is only valid when the corrugation is weak. In our case one justification of this analysis comes from the very good agreement between the measured dispersion of the resonance dips and the results from Eq. (1) based on a free-particle dispersion along the surface. This observation is corroborated by preliminary results from a dynamical analysis based on coupled cannel calculations using a corrugated potential

that is consistent with the observed specular intensity, and the strength and widths of the resonance dips. The calculated shifts and widths in total energy are typically less than 0.1 meV. The large observed widths of the resonance dips seen in Fig. 1 are primarily due to the energy spread of the incident beam. The angular spread also contributes significantly particularly when the dispersion relation is steep. The CMSA resonances appear as dips in the measured specular intensity. This a typical feature related to resonances in the incoming channel in the presence of open channels like diffracted beams or the ubiquitous inelastic channels due to phonons.[11,12]

As first discussed by Le Roy,[8] the Rydberg-Klein-Rees (RKR) method of molecular physics is an elegant tool to decide if a given assignment of the levels is compatible with a single gas-surface potential curve for H_2 and D_2. The RKR method does not assume any prescribed form for the potential and is based on the Wentzel-Kramers-Brillouin (WKB) approximation for the bound state energies ε_n,

$$\eta=\frac{n+\frac{1}{2}}{\sqrt{m}}=\frac{2\sqrt{2}}{h}\int_{z_1}^{z_2}[\varepsilon_z-V_0(z)]^{1/2}dz\ . \tag{2}$$

Here z_1 and z_2 are the classical turning points of the particle with energy ε_z of the motion normal to the surface and mass m in the laterally averaged potential $V_0(z)$ and h is Planck's constant. The bound-state energies ε_n of the potential correspond to integer values of n. In this context the most important feature of this equation is that the energy ε_z as a function of the mass reduced quantum number η is independent of the mass. As a consequence the plots of the corresponding functions for H_2 and D_2 should fall on a single curve for the correct assignment of

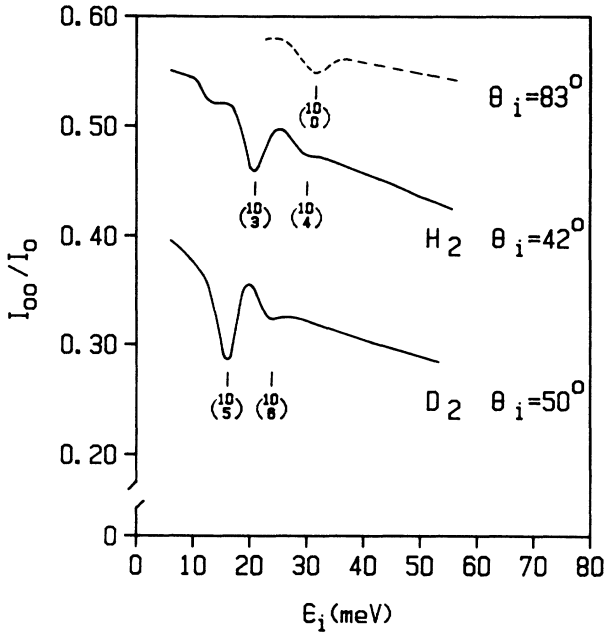

FIG. 1. Specular reflectivity I_{00}/I_0 of H_2 and D_2 from a Cu(100) surface (temperature $\sim$80 K) as a function of incident particle energy ε_i and with incident angles $\theta_i=42°$, 83° (H_2), and 50° (D_2), respectively. I_0 and I_{00} are, respectively, the intensities of the incident and specularly reflected beams. The absolute magnitude of the specular reflectivity for $\theta_i=83°$ has been obtained by an approximate geometric correction accounting for the finite crystal size. The CMSA resonances are labeled by the appropriate G vector (10) and bound-state levels.

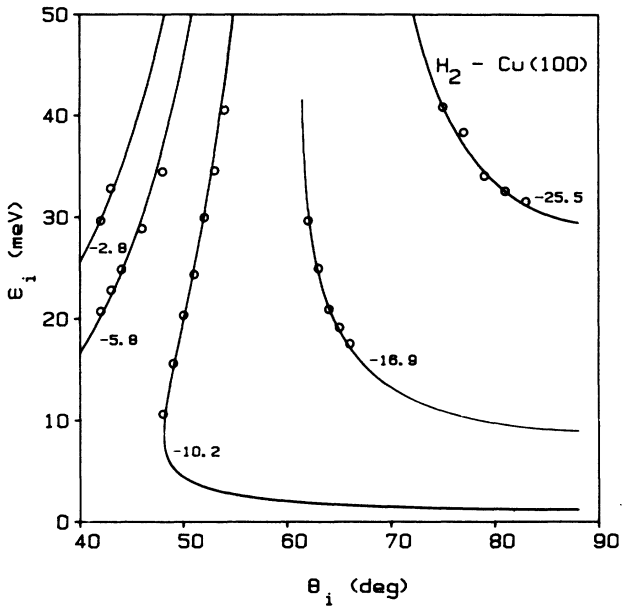

FIG. 2. Dispersion relations for diffractive selective adsorption resonances of H_2 scattered from a Cu(100) surface. Open circles denote measured energies, ε_i of resonance minima vs incident angle θ_i. The solid curves are fitted kinematical free particle dispersion relations denoted by the appropriate bound-state level energies.

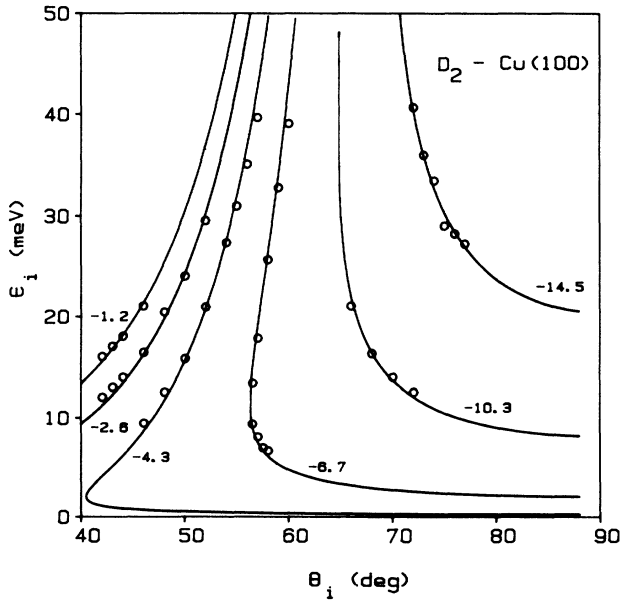

FIG. 3. Dispersion relations for diffractive selective adsorption resonances of D_2 scattered from a Cu(100) surface. Conditions as in Fig. 2.

the bound-state levels. In this context we note that there exist other possible mechanisms that could give rise to isotope effects on the position of the CMSA resonances, e.g., hindering of the free rotation of the adsorbed molecular has been observed on Ag (Refs. 6 and 7) as a sub-meV splitting of CMSA resonances energies of ortho-hydrogen. Changes of the internal zero-point vibrational energy upon adsorption would cause an isotopic shift as recently discussed by Müller.[13] Measured rotational-vibrational spectra for hydrogen molecules adsorbed on Cu(100) (Ref. 2) reveal that this effect is quite small in a physisorption situation. Coupling to the dynamical lattice will also cause isotope effects on ε_n. Estimates based on perturbation theory of the coupling to the Cu(100) phonons show that this effect causes a downwards shift of at most 0.1 meV.[14] In short, these sources of isotope shift are rather small and may be neglected within the error bars inherent in the experiment.

The presence of an attractive van der Waals tail in the potential $V_0(z) \approx -C_{\rm vdW}/z^3$, $z \to \infty$, makes it possible to construct a more informative plot in this case. This kind of asymptotic behavior of the potential introduces a simple relation between $\varepsilon_z(\eta)$ and large η of the form[8]

$$|\varepsilon_z(\eta)|^{1/6} \approx 3.82 C_{\rm vdW}^{-1/3}(\eta_D - \eta) , \quad (3)$$

The prefactor is correct with the units of $\text{amu}^{-1/2}$ for the reduced quantum number, meV for the bound-state energies, and meV a_0^3 for the van der Waals coefficient $C_{\rm vdW}$. η_D is the value of η at the dissociation limit and determines the maximum number of bound states in the potential well. Direct information about the van der Waal coefficient can be extracted from a plot of the inverse sixth power of ε_n with respect to η.

Such plots of the observed bound-state energies are shown in Fig. 4 for H_2 and D_2 for two different assignments of the levels. In the lower plot we have assumed that the lowest H_2 level at -25.5 meV (see fig. 2) is equivalent to the ground-state $n=0$. The figure demonstrates the well-known fact that it is not possible in practice to make a unique assignment from this kind of analysis. Any increase of the level numbers with integers $\Delta n(D_2)$ and $\Delta n(H_2)$, for D_2 and H_2, respectively, such that the rational number $\Delta n(D_2)/\Delta n(H_2)$ is a good approximation to $[m(D_2)/m(H_2)]^{1/2} \approx 1.414$ will also be a compatible assignment due to experimental uncertainties in the energies. In this case an increase with $\Delta n(D_2)=3$ and $\Delta n(H_2)=2$ corresponding to a rational approximate of 1.5 to 1.414 is sufficient to give an almost equally good fit as shown from the figure. However, the well depth increases rapidly with these higher orders of assignments of the levels. The well depth D of the potential is given by the extrapolated values of ε_n to $\eta=0$. A third-order polynomial extrapolation to the H_2 data gives $D \approx 30.90$ meV and $D \approx 60$ meV. We can quite safely rule out the 60-meV well depth as being too large. It would for instance imply a binding energy for the H_2-Cu(100) system that is twice as large as for the H_2-Ag(111) system,[7] which is unrealistic. Furthermore, adsorbed H_2 remains stable on the Cu(100) surface only at a low substrate temperature of ~ 10 K, which is compatible with a 30-meV well depth. It is hard to measure the higher-lying bound-state levels with sufficient accuracy, which makes it difficult to extract an accurate value for $C_{\rm vdW}$ based on Eq. (3). However, an estimate of the slope at $\eta=3$ gives a value $C_{\rm vdW} \approx 5$ eV a_0^3 rather close to the theoretical values reported in the literature $C_{\rm vdW}=4.53$ eV a_0^3 (Ref. 15) and 4.65 eV a_0^3.[16]

From the analysis above we arrive at an H_2-Cu(100) interaction potential with a well depth $D \approx 30.9$ meV. This differs substantially from previously reported values: $D \approx 22.0$ meV for H-Cu(110), Cu(115) (Ref. 4) and $D \approx 22.2$ meV for HD, D_2-Cu(111).[5] We note, however that the problem related to a unique level assignment was recognized in these investigations and possible well depths of 32 meV for Cu(110) and 31.1 meV for Cu(111) were considered but disregarded for various reasons, e.g., with respect to the expected trend in the series of noble metals Cu, Ag, and Au. These latter values are, however, quite close to our determination and definitely support a picture with an H_2-Cu physisorption interaction characterized by $D \approx 31$ meV. This is a most notable result, since it implies that the H_2 interaction potentials for Cu and Ag are very similar.

In Table I we have listed the experimentally observed bound-state levels for H_2 and D_2 interacting with the Cu(100), Ag(111),[7] and Ag(110) (Ref. 6) surfaces. The

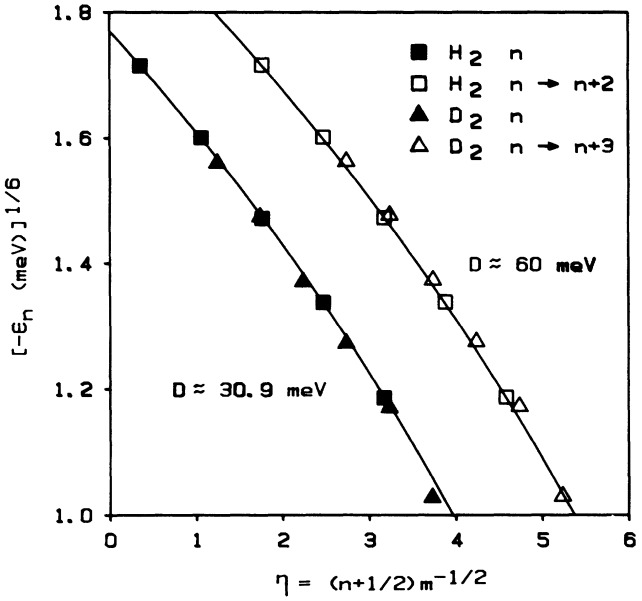

FIG. 4. Le Roy plots of the observed "bound-state" energies. The inverse sixth power of the bound-state energies taken from Figs. 2 and 3 are plotted as a function of the mass reduced level number $\eta=(n+1/2)/\sqrt{m}$. The solid symbols are the results for the new assignment of the levels proposed in this paper. An alternative assignment shown by the open symbols based on changing the level numbers by 3 for D_2 and 2 for H_2, respectively, gives almost as good fit to the data. However, the latter fit gives rise to a well depth about 60 meV as compared to 30.9 meV. These two well depths have been infered from third-order polynomial fits to the H_2 data as indicated by the thin lines.

TABLE I. Bound-state levels of H_2 and D_2 on Cu and Ag. The bound-state energies ε_n listed under columns labeled "Theory" correspond to an exp(−3) potential, Eq. (4), and are all taken from Nordlander, Holmberg, and Harris (Ref. 9). The theoretical data are quoted for the Cu(110) since the data for Cu(100) surface (Ref. 17) are only preliminary. An extra interpolation of the potential parameters as a function of the work function gives a potential for Cu(100) that differs at most with 0.1 meV from Cu(110) for the bound-state energies. The results from a more accurate calculation of the repulsive parameters give about same differences between the level sequences for Cu and Ag (Ref. 18). The experimental data are extracted from measurements of corrugation-mediated selective adsorption resonances (CMSA). The experimental data for Ag(111) are for para-H_2 and ortho-D_2 ($J=0$) and the experimental data for Ag(110) are for para-H_2 and the rest for normal hydrogen. All energies are in meV.

	Experiment		ε_n	Theory	
n	Cu(100)[a]	Ag(111)[b]	Ag(110)[c]	Cu(110)	Ag(111)
			H_2		
0	−25.5±0.2	−25.74±0.07	−25.9±0.4	−19.9	−23.8
1	−16.9±0.2	−16.87±0.07	−16.4±0.2	−11.9	−15.2
2	−10.2±0.2	−10.11±0.09	−10.0±0.2	−6.8	−9.2
3	−5.8±0.2	−5.47±0.1	−5.4±0.3	−3.5	−5.0
4	−2.8±0.2	−2.61±0.13	−2.7±0.3	−1.6	−2.5
5		−1.21±0.06	−1.1±0.3	−0.6	−1.1
			D_2		
0			−27.5±0.3		
1			−20.0±0.3		
2	−14.5±0.2	−14.47±0.2	−14.3±0.3		
3	−10.3±0.2	−10.09±0.06	−9.8±0.1		
4	−6.7±0.2	−6.57±0.1	−6.3±0.1		
5	−4.3±0.2	−3.97±0.06	−3.8±0.2		
6	−2.6±0.2	−2.39±0.1	−2.0±0.2		
7	−1.2±0.2	−1.13±0.06	−0.7±0.2		

[a]This work.
[b]Reference 7.
[c]Reference 6.

close correspondence between the Cu and Ag data is striking and quite intriguing when put in perspective with recent theoretical calculations. We note that the H_2-Cu(110), Cu(115) data,[4] and the D_2-Cu(111) data[5] also agree with this pattern provided we shift the assumed level assignment one step upwards.

The calculated ε_n in Table I are based on a theory where the potential well is formed by the delicate balance between the attractive van der Waals potential and the potential wall created by the Pauli repulsion. The resulting potential can be approximated by the exp(−3) form,[9]

$$V_0(z)=V_0\exp(-\alpha z)-\frac{C_{\mathrm{vdW}}}{(z-z_{\mathrm{vdW}})^3}f[k_c(z-z_{\mathrm{vdW}})]\ , \tag{4}$$

where V_0 is a repulsive potential parameter, α is the repulsive exponent, C_{vdW} and z_{vdW} are the van der Waals parameters, and k_c is a cutoff parameter. The function $f(x)=1-[2x(1+x)+1]e^{-2x}$ describes the saturation of the van der Waals attraction due to the finite size of the molecule.

A general trend in the calculated physisorption interaction of H_2 with noble metals is the increasing well depth in the series Cu, Ag, and Au.[9] This behavior is reflected in the theoretical ε_n values listed in Table I; the low-lying Ag levels are about 25% below the corresponding Cu levels. The experimental data, on the other hand, show only minute differences. A closer scrutiny of the calculations of the potential parameters points to several factors that may contribute to the disagreement show in Table I.

The calculated values for C_{vdW} reported in the literature do not agree on the trend over the noble metals both for He and H_2. Using the values suggested by Schwartz and Le Roy[15] instead of the values given by Persson and Zaremba[16] brings down the difference in well depths from being 23.6 and 28.9 meV to 24.6 and 26.3 meV for H_2 on Cu(110) and Ag(111), respectively. Another source of uncertainty is that the potential minima occurs rather close to the surface which makes the well depth quite sensitive to how the saturation of the van der Waals attraction is modeled. An increase of k_c from 0.4 to 0.45 deepens the latter well depths to 29.9 and 32.5 meV for Cu and Ag, respectively, quite close to the values 30.9 and 31.5 meV suggested by an analysis of the experimental data for Cu(100) and Ag(111),[7] respectively. A minor adjustment of the van der Waals parameters so that the observed ε_0 for H_2 is reproduced for Cu(100) and Ag(111), respectively, give a good agreement between the observed and calculated level sequences as tabulated in Tables I and II

TABLE II. Calculated bound-state levels for hydrogen on Cu and Ag. The bound-state levels have been calculated numerically for an exp(−3) potential given by Eq. (4) using different adjustments of the potential parameters given by Nordlander, Holmberg, and Harris (Ref. 9) for Cu(110) and Ag(111), respectively. The result tabulated in the columns labeled "Attractive part" corresponds to a change of k_c from $0.4a_0^{-1}$ to $0.45a_0^{-1}$ and using $C_{vdW}=4.74$ eV a_0^3 and 4.46 eV a_0^3 for Cu and Ag, respectively. The latter values are minor modifications of the values suggested by Schwartz and Le Roy (Ref. 15) ($C_{vdW}=4.65$ eVa_0^3 and 4.56 eVa_0^3) instead of the original values given by Persson and Zaremba (Ref. 16). The results tabulated in the columns labeled by "Repulsive part" correspond only to an adjustment of V_0 to 3.50 and 4.07 eV for Cu and Ag, respectively, and keeping the rest of the potential parameters to their original values. The same procedure applied to the attractive and repulsive parts of the potential when starting from the new set of repulsive parameters (Ref. 18) gives a poorer agreement with the observed level sequences when comparing both Cu and Ag. All energies are in meV.

	Cu(100)		ε_n	Ag(111)
n	Attractive part	Repulsive part	Attractive part	Repulsive part
		H_2		
0	−25.54	−25.49	−25.76	−25.78
1	−16.66	−16.76	−16.74	−17.01
2	−10.08	−10.23	−10.07	−10.44
3	−5.55	−5.69	−5.49	−5.87
4	−2.73	−2.82	−2.66	−2.96
5			−1.12	−1.31
		D_2		
0	−27.04	−27.0	−27.28	−27.26
1	−20.27	−20.3	−20.40	−20.58
2	−14.68	−14.81	−14.73	−15.04
3	−10.22	−10.37	−10.21	−10.58
4	−6.78	−6.94	−6.74	−7.12
5	−4.27	−4.40	−4.21	−4.56
6	−2.53	−2.62	−2.47	−2.75
7	−1.41	−1.46	−1.35	−1.55

both for H_2 and D_2. In the case of He the potential well is virtually insensitive to k_c. The calculated sequences of $\varepsilon_n=-3.9$, -1.9, -0.74, and -0.1 meV for Cu(110) (Ref. 19) and $\varepsilon_n=-5.3$, -2.9, -1.4, and -0.5 meV for Ag(110) (Ref. 19) show similar disagreement with the observed sequences $\varepsilon_n=-4.45$, -2.1, -0.9, and -0.35 meV for Cu(115) (Ref. 4) and -4.44, -2.18, -0.92, -0.31, and -0.095 meV for Ag(110).[20] Note again the striking agreement between the observed level sequences for Cu and Ag. Also in this case the difference in the calculated well depths would decrease if the values for C_{vdW} suggested by Schwartz and Le Roy[15] were used.

The repulsive part is constructed from a pseudopotential expansion and the results are sensitive to the behavior of the tails of the electron wave functions. For instance, the decay of the wave functions determines the repulsive exponent and is governed by the work function Φ. The calculations of Nordlander, Holmberg, and Harris[9] use a modified jellium description of the noble metals—a modification that is introduced to approximately correct for the fact that a jellium model does not correctly reproduce the work functions of the noble metals. A piece of evidence that this modification might not be sufficient is that the observed D_2 bound-state levels for Cu(111) (Ref. 5) using the new assignment $\varepsilon_n=-9.3$, -6.4, -4.1, and -2.4 meV, $n=3$, 4, 5, and 6, lie slightly higher than for Cu(100). This is not in accordance with expectation since the larger Φ of the (111) surface would give rise to a steeper repulsive wall and accordingly a deeper well. This fact allows us to investigate the effects of changes of V_0 on $V_0(z)$, keeping the original values for the van der Waals parameters. Adjusting V_0 so that the observed ε_0 for H_2 is reproduced indeed gives level sequences for Cu(100) that are in excellent agreement with the observed ones (see Tables I and II) both for H_2 and D_2. The same tables shows also that a corresponding adjustment of V_0 for Ag(111) does not result in an equally good agreement, however.

Our discussion shows that based on the potential form given in Eq. (4) we are not able from the analysis of the experimental data to arrive at a unique set of potential parameters for Cu and Ag. A more refined treatment of the electron structure of the noble metals is needed in the modeling of the attractive and repulsive part of the physisorption interaction to resolve this problem and in order to understand the trends over the noble metals and different crystal orientations.

IV. SUMMARY

In summary, we have measured bound-state level sequences for H_2 and D_2 on Cu(100) that are compatible with a single gas-surface potential curve. We noted that the well depth, 30.9 meV, is surprisingly close to the

values 31.5–31.7 meV reported for the H_2-Ag system. This close correlation between the physisorption interaction of H_2 with Cu and Ag surfaces is not corroborated by recent theoretical calculations. These calculations are based on a division of the physisorption potential into a part due to van der Waals attraction and a part due to Pauli repulsion. This approach has been successful in understanding the differences in well depths between He and H_2 on metal surfaces. More subtle details in the description of the physisorption interaction, such as the trends over the noble metals and different surface orientations, appear to require refined treatments of the van der Waals constants and the substrate electron structure. There is no doubt, however, that the approximated $\exp(-3)$ form of the potential gives a very good description of the bound-state levels if the relevant parameters are adjusted properly.

ACKNOWLEDGMENTS

We thank our collegues J. Harris and R. Ryberg for numerous valuable discussions. Financial support from the Swedish Natural Science Research Council (NFR) is also gratefully acknowledged.

[1]Ph. Avouris, D. Schmeisser, and J. E. Demuth, Phys. Rev. Lett. **48**, 199 (1982).
[2]S. Andersson and J. Harris, Phys. Rev. Lett. **48**, 545 (1982).
[3]A.-S. Mårtensson, C. Nyberg, and S. Andersson, Phys. Rev. Lett. **57**, 2045 (1986).
[4]J. Perrau and J. Lapujoulade, Surf. Sci. **121**, 341 (1982).
[5]U. Harten, J. P Toennies, and Ch. Wöll, J. Chem. Phys. **85**, 2249 (1986).
[6]M. Chiesa, L. Mattera, R Musenich, and C Salvo, Surf. Sci. **151**, L145 (1985).
[7]C.-F. Yu, K. B. Whaley, C. S. Hogg, and S. J. Sibener, Phys. Rev. Lett. **51**, 2210 (1983); J. Chem. Phys. **83**, 4217 (1985).
[8]R. J. Le Roy, Surf. Sci. **59**, 541 (1976).
[9]P. Nordlander, C. Holmberg, and J. Harris, Surf. Sci. **175**, L753 (1986).
[10]E. Zaremba and W. Kohn, Phys. Rev. B **15**, 1769 (1977).
[11]V. Celli and D. Evans, in *Dynamics of Gas-Surface Interactions*, edited by G. Benedek and U. Valbusa (Springer-Verlag, Berlin, 1982), p. 2.
[12]J. G. Mantovani, J. R. Mason, and G. Armand, Surf. Sci. **143**, 536 (1984).
[13]J. E. Müller, Phys. Rev. Lett. **59**, 2943 (1987).
[14]M. Persson, Phys. Rev. B **36**, 7870 (1987).
[15]C. Schwartz and R. J. Le Roy, Surf. Sci. **166**, L141 (1986).
[16]B. N. J. Persson and E. Zaremba, Phys. Rev. B **30**, 5669 (1984).
[17]J. Harris and A. Liebsch, Phys. Scripta, **T4**, 14 (1983).
[18]P. Nordlander, C. Holmberg, and J. Harris, Surf. Sci. **152**, 702 (1985).
[19]P. Nordlander and J. Harris, J. Phys. C **17**, 1141 (1984).
[20]M. G. Dondi, L. Mattera, S. Terreni, F. Tommasini, and U. Lincke, Phys. Rev. B **34**, 5897 (1986).